

# Distributed MPC for Thermal Comfort and Load Allocation with Energy Auction

F. A. Barata<sup>\*‡</sup>, J. M. Igreja<sup>\*</sup>, Rui Neves-Silva<sup>\*\*</sup>

<sup>\*</sup>Department Area of Electrical Engineering and Automation, Instituto Superior de Engenharia de Lisboa, ISEL/IPL, R. Conselheiro Emídio Navarro n°1, 1959-007 Lisboa Portugal

<sup>\*\*</sup> Department of Electrical Engineering, FCT / UNL, 2829-516 Monte da Caparica, Portugal

(fbarata@deea.isel.ipl.pt, jigreja@deea.isel.ipl.pt, rms@fct.unl.pt)

<sup>‡</sup>Corresponding Author; F. A. Barata, R. Conselheiro Emídio Navarro, 1959-007, Lisboa Portugal, +351 21 831 7010, fbarata@deea.isel.ipl.pt

*Received: 21.03.2014 Accepted: 02.06.2014*

**Abstract-** This paper presents a distributed predictive control methodology for indoor thermal comfort that optimizes the consumption of a limited shared energy resource using an integrated demand-side management approach that involves a power price auction and an appliance loads allocation scheme. The control objective for each subsystem (house or building) aims to minimize the energy cost while maintaining the indoor temperature inside comfort limits. In a distributed coordinated multi-agent ecosystem, each house or building control agent achieves its objectives while sharing, among them, the available energy through the introduction of particular coupling constraints in their underlying optimization problem. Coordination is maintained by a daily *green* energy auction bring in a demand-side management approach. Also the implemented distributed MPC algorithm is described and validated with simulation studies.

**Keywords** DMPC; limited *green* energy resource; energy auction, DSM; load shifting allocation.

## 1. Introduction

Nowadays buildings spend 40% of the world's energy production and are responsible by almost 50% of the total of greenhouse gas emissions. Therefore, buildings produce more greenhouse gases than traffic and industry, which is estimated at 31% and 28%, respectively [1]. This fact is mainly due the intensification of energy consumption in HVAC systems to satisfy the demand for thermal comfort [2], making it the largest energy end use both in the residential and non-residential sector, covering heating, ventilation and air conditioning [3]. Consequently, it is economically, socially, and environmentally important to reduce the energy consumption and increase the efficiency of buildings.

The approach here presented intends to take advantage from the innovative technology characteristics provided by future Smart Grids (SGs) [4]. In the smart world, simple household appliances, like dishwashers, clothes dryers, heaters, air conditioners will be fully controllable in order to achieve maximum efficiency. Active Demand-Side Management (DSM) in SGs [5] will control the loads in order to adapt them to the availability of the existing

renewable energy sources. The important role of DSM in the future distributed SGs is discussed in [6, 7]. DSM studies are focused in the development of load control manipulation models [8, 9], and electricity incentive prices to promote load management [10, 11]. In buildings, DSM is based on an effective reduction of the energy needs by changing the shape and amplitude consumers load diagram. The DSM can involve a combination of several strategies, pricing, load curves management and other approaches of energy conservation aiming for one more energy efficient use.

Load shifting is already a common practice of managing electricity supply and demand in order to avoid the energy peaks periods. Load shifting allows improving energy efficiency and reducing emissions by smoothing the daily demand curve with the decrease of peaks and valleys in the demand profile. In the residential sector recent papers provide interesting state of the art architectures and different approaches for load shifting simulation models [10, 13, 14]. Remark that demand-side management approaches must provide control and allocate different types of appliances, such as air conditioners, refrigerators, water heaters, heat pumps or others, to the most appropriate time.

In particular, allocation schemes allow smart appliances shift their operation to the hours that most benefit the consumers. This kind of procedure ensures that at the same time, the smart appliance is turned on when the renewable resource is available, and consequently the energy price is lower, while the indoor comfort is maintained. In an integrated approach the system will minimize the consumer energy costs by maximizing the use of renewables adjusting the demand to the available resources. The profile of delivered energy depends on several factors, such as price of conventional energy and availability of renewable energy.

Model Predictive Control (MPC) has been granted to reduce and optimize the energy consumption in the residential sector namely to deal with temperature set points regulations [15, 16, 17, 18] when compared with the conventional PI controllers [19]. MPC can provide a potential building energy saving of 16–41%, with the additional advantage of include robustness, adjustment and flexibility [20] against the commonly used HVAC controllers. A survey about the MPC features in the field of advanced HVAC control can be seen in [21].

The MPC have also evolved as a distributed systems control methodology [22, 23, 24]. Distributed Model Predictive Control (DMPC) allows the distribution of decision-making while handling constraints in a systematic way. DMPC strategies can be characterized by the type of couplings or interactions assumed between component subsystems also known as agents [25, 26].

DMPC is better understood in a Multi Agent System (MAS) context, where distributed infrastructures are dynamically interconnected and control by multiple agents that share information among them. In this case each agent represents a thermal control area (TCA), that belongs to a group of distributed, autonomous analogous entities within an environment, where they can act and react in order to work together to achieve a common goal [27, 28, 29].

This work contributes, in a model predictive control multi-agent systems context, with an integrative methodology to manage networks from the demand side with strong presence of intermittent energy sources. This methodology involves a power price auction plus an appliance loads allocation scheme, where, subsystems share among them the available energy aiming each one to minimize their energy cost while maintaining the indoor temperature within the comfort zone. The coordination between agents is established by a daily *green* energy auction. This auction mechanism provides a sequential access scheme, in a distributed scenario for interconnected linear time-invariant multi-agent MPC systems. The scheme is formulated for multi-zone dynamically coupled areas that are also coupled by energy constraints, perceived as TCAs. The inclusion of all the referred features, in one integrated DMPC solution, to the best knowledge of the authors of this article, makes this work be original.

The paper is organized as follows. Section 2 presents the global system overview, which includes the overall distributed scenario, the TCA models, the DMPC formalization and implemented algorithm. Section 3

illustrates the solution approach with simulation results and in Section 4 some conclusions and future work are discussed.

## 2. Overall system overview

In this section the distributed scenario and the demand-side approach assumptions are introduced along with the thermal dynamical models needed for control prediction.

### 2.1. Distributed scenario

The scenario built considers a distributed network that involves a residential community, with electricity power source generated by their own renewable energy park. Hereafter the term house is used to designate any type of space for human accommodation like house, offices, buildings and other types of similar constructions.

The set of houses defined by  $W = \{w_1, w_2, \dots, w_{N_w}\}$  may have several divisions  $D_l = \{d_{l1}, d_{l2}, \dots, d_{lnd}\}$  and  $l = 1, \dots, N_w$ , remark that with  $N_d=1$  the house is represented by one division. Each division may have different thermal loads, thermal characteristics, occupancy and comfort temperature bounds, and consequently with different energy needs for heating/cooling the spaces.

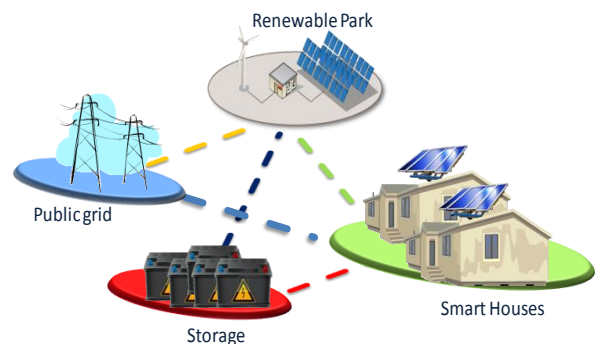


**Fig. 1.** Implemented scheme.

The *green* resource is shared through the following auction scenario. Each house has a known fixed 24 hours consumption profile,  $C_{w_{it}}(k)$  and it is established a priority level from 1 (low) to 3 (high) for each hour to indicate how important is to have available resource to supply the load. The bid value of each house is made according the chosen priority level, the hours with high priority levels indicates high consumption and consequently a higher bid value. The agents make their bid in the auction (more details about the auction algorithm can be seen in previous work [30]) with one day ahead to show how much intend to pay per kWh to consume the *green* resource in each one of the next 24 hours. Thus, the access to the *green* resource is done hourly according to the bid value made. The one that is able to pay more uses the needed stock first and the second can use only the remainder energy, and so on. The *red* resource (from grid) has a fixed kWh price that is always higher than the *green* to promote the renewable energy consumption. The available *green* resource can be stored in batteries up to capacity value ( $B_{cv}$ ), when reached it is considered that the remaining *green* resource is delivered to the grid.

The sliding load scheme begins by each division selecting the load value ( $L_V$ ), the duration ( $L_{Vd}$ ), the turned on time ( $T_{OT}$ ) and the "sliding level" ( $S_L$ ) of one/two "shifted loads". The  $S_L$  indicates that the load can be turned on  $S_L$  hours before and after the chosen  $T_{OT}$ . The next picture illustrates the shifting load characteristics.

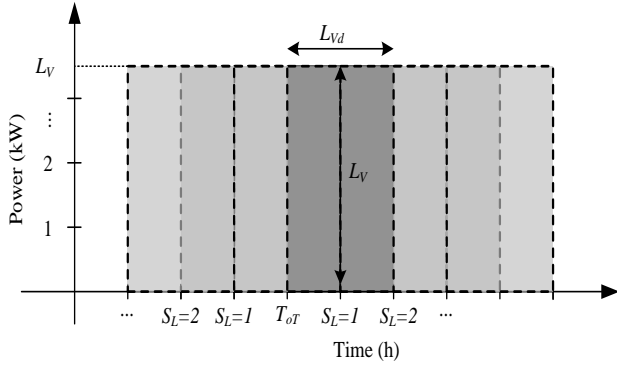


Fig. 2. Shifting load characteristics.

Therefore, using the demand side management, by negotiating the energy price and the consumer comfort, the distributed loads can be allocated in order to guarantee that all constraints are satisfied.

The overall system scenario includes an auction (provided by the market operator) that, according to the bid value made by the agent defines an order to access to the green energy. The green resource consumption is made by the agents sequentially by the auction order, and the information about the remainder green resource is passed to the next agent as the maximum green available resource. As mentioned, when the green resource becomes insufficient to satisfy all the demand, the red is available.

The main objective is to find a distributed predictive control law to maintain the temperature and power consumption according to the described scenario.

## 2.2. Thermal models

House models can be simple or more complex depending on the goal to be achieved. In this paper, a first order energy balance model (1-3) is used to describe the dominant dynamics of a generic division. Remark that these are the basic equations for edifice thermal modelling that can be described by several divisions and floors that can thermally interact between them.

$$\frac{dT_l}{dt} = \frac{1}{C_l} (Q_{heatl} - Q_{losseq} + Q_{Pd_l}), \quad (1)$$

$$Q_{losseq} = \frac{T_{out} - T_l}{R_{eq_l}} + \sum_{g=1}^{Nar} \frac{T_g - T_l}{R_{lg}}, \quad (2)$$

$$R_{eq_l} = R_{roof_l} // R_{window_l} // R_{wall_l} // R_{th_l}, \quad (3)$$

$$R_{window_l} = \sum R_{window_{materials}},$$

$$R_{roof_l} = \sum R_{roof_{materials}},$$

$$R_{wall_l} = \sum R_{wall_{materials}}$$

where in (1),  $Q_{losseq}$  is heat and cooling losses from a generic division  $l$  (kW),  $T_l$  the inside temperature ( $^{\circ}C$ ),  $C_l$  the equivalent thermal capacitance (kJ/ $^{\circ}C$ ), and  $Q_{heatl}$  the heat and cooling power (kW) and  $Q_{Pd_l}$  the external thermal disturbances (kW) (e.g. load generated by occupants, direct sunlight, electrical devices or doors and windows aperture to recycle the indoor air). In (2)  $T_{out}$  is the outdoor temperature ( $^{\circ}C$ ),  $R_{lg}$  the thermal resistance between division  $l$  and the adjacent zones  $g$ ,  $R_{eq_l}$  the equivalent thermal resistance and  $R_{th_l}$  the air thermal resistance to bulk of division. Figure 3 shows the electrical equivalent of division model (1-3). For a complete thermal model see [31] and the example for a whole house in annexe.

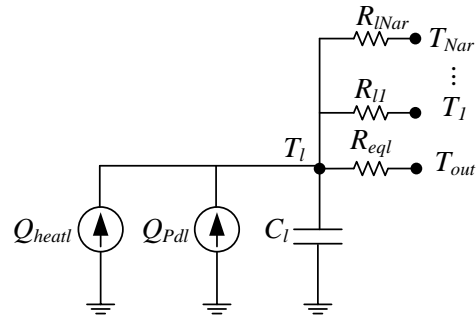


Fig. 3. Generic schematic representation of thermal-electrical modular analogy for one division  $l$  with  $Nar$  adjacent zones.

Discrete model space-state representation of (1-3) can be generalized for one house, with several divisions, using Euler discretization [32] with a sampling time of  $\Delta t$ , by

$$T_{il}(k+1) = A_{il}T_{il}(k) + B_{il}u_{il}(k) + \sum_{g=1}^{Nar} A_{ig}T_{ig}(k) + v_{il}(k), \quad (4)$$

$$\text{where } A_{il} = \left( 1 - \frac{R_{eq_l} + R_{lg}}{R_{eq_l} C_{il}} \Delta t \right), B_{il} = \frac{\Delta t}{C_{il}},$$

$$D_{il} = \sum_{g=1}^{Nar} \frac{T_{ig}}{C_{il} R_{il}} \Delta t, v_{il} = \frac{P_{d_{il}} \Delta t}{C_{il}} + \frac{T_{oa} \Delta t}{R_{eq_l} C_{il}}.$$

Inputs  $u_{il}(k)$  are the heat/cooling power to provide comfort in a generic house  $i$  division  $l$ ,  $T_{il}(k)$  is the indoor temperature,  $v_{il}(k)$  is a disturbance signal resulting from the external disturbances (kW) (e.g. load generated by occupants, direct sunlight, electrical devices or doors and windows aperture to recycle the indoor air), and  $T_{oa}$ , the temperature of outside air ( $^{\circ}C$ ).

Figure 4 shows an example for eight divisions divided into four houses or TCAs:  $W = \{w_1, w_2, w_3, w_4\}$  where the zones that thermally interact are not only dynamically

coupled but can be also coupled by power constraints as explained in the sequel.

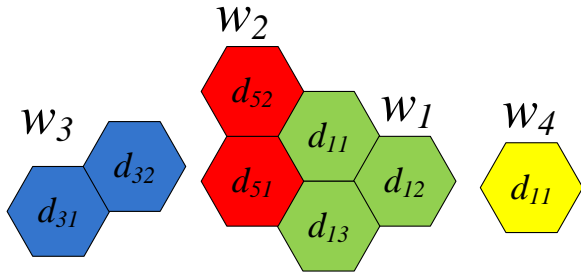


Fig. 4. Generalized house scheme example.

Remark that complex models including several houses can always be represented by a space state LTI model, up the some degree of complexity, given by

$$x(k+1) = Ax(k) + Bu(k) + V(k), \quad (5)$$

where  $x(k)$  represents the state variables, e.g. division temperatures vector,  $u(k)$  is the input vector, heat/cooling power units, and  $v(k)$  collects the thermal disturbances in a vector.

### 2.3. DMPC formalization

The main goal is to ensure thermal comfort with minimal energy consumption, thus the MPC cost function must be mathematically formulated having into account this objective and simultaneously maintaining the room temperature inside the comfort range using all the available *green* energy. Remark that at each time step, each agent  $i$  must solve his own MPC optimization problem. Specifically, the combined goals are: i) minimize the energy consumption, heating and cooling; ii) minimize the peak power consumption; iii) maintain the desired temperature range and iv) use all the *green* power available minimizing at the same time the *red* energy consumption.

The optimization problem formulation to be solved by each agent at each instant, assumes the following form:

$$\min_{U, \bar{\varepsilon}, \underline{\varepsilon}, \bar{\gamma}, \underline{\gamma}} J_i(k) = \sum_{j=0}^{H_p-1} \left[ \sum_{l=1}^{Nd_i} u_{il}(k+j)^T R_{il} u_{il}(k+j) \right] + \sum_{l=1}^{Nd_i} \phi_l \max \{ u_{il}^2(k), \dots, u_{il}^2(k+H_p-1) \} + \sum_{j=1}^{H_p} \left[ \sum_{l=1}^{Nd_i} \left( \varepsilon_{il}(k+j)^T \Xi_{il} \varepsilon_{il}(k+j) + \gamma_{il}(k+j)^T \Psi_{il} \gamma_{il}(k+j) \right) \right] \quad (6)$$

$$\min_{U_i, \varepsilon_i, \gamma_i} J_i(k) = \varepsilon_i^T(k) \Xi_i \varepsilon_i(k) + \gamma_i^T(k) \Psi_i \gamma_i(k) + U_i^T(k) R_i U_i(k) + \sum_{l=1}^{Nd_i} \phi_l \max \{ u_{il}^2(k), \dots, u_{il}^2(k+H_p-1) \}, \quad (7)$$

with,

$$U_i(k) = \begin{bmatrix} U_{i1}(k) \\ U_{i2}(k) \\ \vdots \\ U_{iNd}(k) \end{bmatrix}, \quad (8)$$

$$\varepsilon_i(k) = \begin{bmatrix} \bar{\varepsilon}_{i1}(k) \\ \bar{\varepsilon}_{i2}(k) \\ \vdots \\ \bar{\varepsilon}_{iNd}(k) \\ \underline{\varepsilon}_{i1}(k) \\ \underline{\varepsilon}_{i2}(k) \\ \vdots \\ \underline{\varepsilon}_{iNd}(k) \end{bmatrix}, \quad \bar{\varepsilon}_{ii}(k) = \begin{bmatrix} \bar{\varepsilon}_{ii}(k+1) \\ \bar{\varepsilon}_{ii}(k+2) \\ \vdots \\ \bar{\varepsilon}_{ii}(k+H_p) \end{bmatrix}, \quad \underline{\varepsilon}_{ii}(k) = \begin{bmatrix} \underline{\varepsilon}_{ii}(k+1) \\ \underline{\varepsilon}_{ii}(k+2) \\ \vdots \\ \underline{\varepsilon}_{ii}(k+H_p) \end{bmatrix}, \quad (9)$$

$$\gamma_i(k) = \begin{bmatrix} \bar{\gamma}_i(k) \\ \underline{\gamma}_i(k) \end{bmatrix}, \quad \bar{\gamma}_i(k) = \begin{bmatrix} \bar{\gamma}_i(k+1) \\ \bar{\gamma}_i(k+2) \\ \vdots \\ \bar{\gamma}_i(k+H_p) \end{bmatrix}, \quad \underline{\gamma}_i(k) = \begin{bmatrix} \underline{\gamma}_i(k+1) \\ \underline{\gamma}_i(k+2) \\ \vdots \\ \underline{\gamma}_i(k+H_p) \end{bmatrix}. \quad (10)$$

Resulting in quadratic optimization problem in the compact form

$$\min_{Z_i} J_i(k) = Z_i^T \Theta Z_i + \sum_{l=1}^{Nd_i} \phi_l \max \{ u_{il}^2(k), \dots, u_{il}^2(k+H_p-1) \} \quad (11)$$

with

$$Z_i = \begin{bmatrix} U_i \\ \varepsilon_i \\ \gamma_i \end{bmatrix}, \quad \Theta = \begin{bmatrix} R_i & 0 & 0 \\ 0 & \Xi_i & 0 \\ 0 & 0 & \Psi_i \end{bmatrix}, \quad (12)$$

and subject to the following constraints

$$X_{il}(k+j+1) = A_{il} X_{il}(k+j) + B_{il} u_{il}(k+j) + \sum_{\substack{g=1 \\ (g \neq l)}}^{Nd_i} A_{ig} X_{lg}^P(k+j) + v_{il}(k+j), \quad (13)$$

( $j = 1, \dots, H_p$ ),

$$\underline{T}_{il}(k+j) - \underline{\varepsilon}_{il}(k+j) \leq T_{il}(k+j) \leq \bar{T}_{il}(k+j) + \bar{\varepsilon}_{il}(k+j), \quad (14)$$

$$\underline{U}_{il}(k+j-1) - \underline{\gamma}_{il}(k+j-1) \leq \sum_{l=1}^{Nd_i} U_{il}(k+j-1) \leq \bar{U}_{il}(k+j-1) + \bar{\gamma}_{il}(k+j-1), \quad (15)$$

$$\underline{\gamma}_i, \bar{\gamma}_i, \underline{\varepsilon}_{il}, \bar{\varepsilon}_{il} \geq 0. \quad (16)$$

In (6),  $Nd_i$  is the number of divisions of house  $i$ ,  $u_{il}$  represents the power control inputs from house  $i$  division  $l$ ,  $\phi_i$  is the penalty on peak power consumption,  $\Xi_i$  is the penalty on the comfort constraint violation,  $\Psi_i$  the penalty on the power constraint violation and  $H_P$  is the length of the prediction horizon. Equation (13) models the house dynamics. Constraints (14) and (15) are *soft constraints*. In (14),  $\varepsilon_{il}$  and  $\bar{\varepsilon}_{il}$  are the vectors of temperature violations that are above and below the desired comfort zone defined by  $T_{il}$  and by  $\bar{T}_{il}$ . In (15),  $\gamma_i$  and  $\bar{\gamma}_i$  are the power violations slack variables when the limits imposed by  $\bar{U}_i$  and  $\underline{U}_i$  are exceeded. Remark that the maximum available green power for house  $i$  at instant  $k$  is  $\bar{U}_i$  given by (19), and minimum,  $\underline{U}_i = -\bar{U}_i$ .

#### 2.4. Shifting loads approach and implemented algorithm

Each one of the systems starts by choosing their loads characteristics,  $L_v$ ,  $L_{vd}$ ,  $T_{oT}$  and  $S_L$ . With this data, all the possible loads schedule combinations ( $PLSC_s$ ) are established (see Fig. 8 e.g.). At each time step, it's verified if inside the predictive horizon, any  $PLSC_s$  exceeds the maximum available  $\bar{U}L_i$ . The sequences that are at any instant above the  $\bar{U}L_i$  limit are removed, and the remaining are the feasible load schedule combinations ( $FLSC_s$ ) resulting in a set of combinations  $\bar{U}_i$  that are tested in the minimization problem as maximum available green resource for comfort (6). The hypothesis that provided less consumption is chosen. Once one sequence is started, all the others that are different until the current step time are eliminated until the final load sequence is chosen,  $FLSeq$ . The total consumption by division and house at any instant can be written as (17) and (18) respectively. Remark that the total available for comfort for each house (19) is used as constraint in the optimization problem. The equations assume the following form,

$$P_{il}(k) = |u_{il}(k)| + Cw_{il}(k) + FLSeq_{il}(k), \quad (17)$$

$$P_i(k) = \sum_{l=1}^{Nd_i} P_{il}(k), \quad (18)$$

$$\bar{U}_i(k) = \bar{U}_{T_{green}}(k) - \sum_{l=1}^{Nd_i} (Cw_{il}(k) - FLSeq_{il}(k)) - \sum_{\substack{j=1 \\ i \neq j}}^{N_W} P_j(k). \quad (19)$$

A simplified scheme of the implemented optimization problem is shown in the next picture, Fig. 5, followed by the implemented DSM-DMPC.

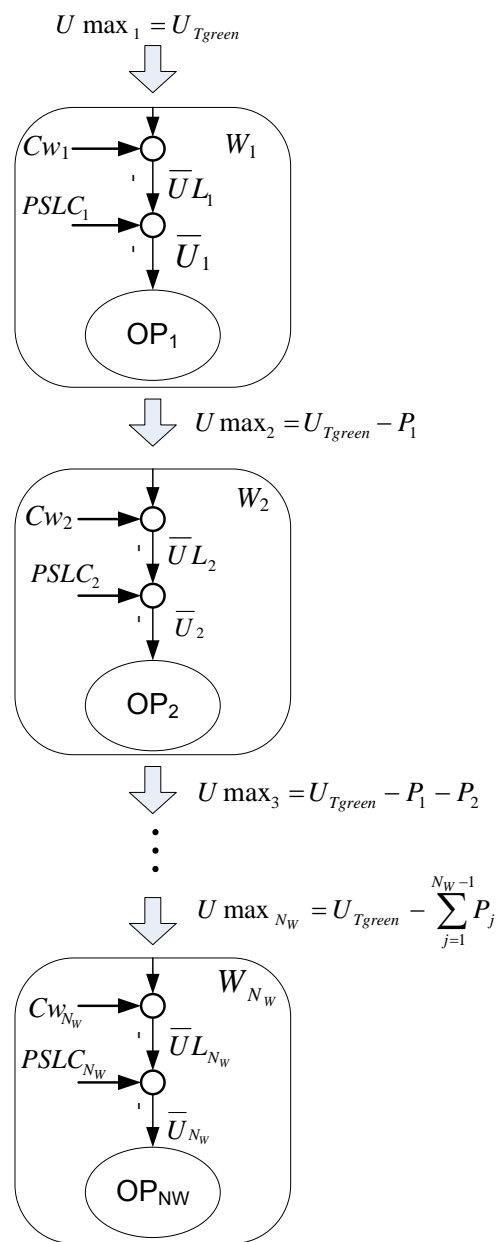


Fig. 5. Implemented power distribution scheme starting in the Optimization Problem 1 (OP<sub>1</sub>) to OP<sub>N<sub>W</sub></sub>.

<b>DSM-DMPC pseudocode prototype algorithm</b>	
For all houses $W_i$ initialize:	
$L_V$	load value
$L_{Vd}$	the duration
$T_{oT}$	the turned on time
$S_L$	sliding level
$PSLC_i$	possible schedule loads combinations ( $n_{PC} \times H_p$ ) with $n_{PC}$ the number of possible combinations
$Cw_{it}$	fixed consumption within $H_p$ ( $1 \times H_p$ )
$B_V$	bid value by hour inside the $H_p$ ( $1 \times H_p$ )
$A_O$	access order to <i>green</i> resource is established within the $H_p$ ( $N_w \times H_p$ ).
<b>for k=1...<math>H_C</math></b>	
<b>for i=1 to <math>N_w</math> (the number of houses, agents)</b>	
<b>Get the access order at current instant, <math>A_O(k)</math></b>	
<b>Get <math>T_{it}(k)</math> (given by eq. (4))</b>	
<b>Calculate <math>\bar{U}L_i(k : k + H_p) \leftarrow \bar{U} \max_i(k : k + H_p) - \sum_{t=1}^{Nd_i} C_{it}(k : k + H_p)</math></b>	
<b>Built table with all <math>FLSC_S</math></b>	
<b>if <math>\bar{U}L_i(k : k + H_p) - PSLC_i(n_{PC}, k : k + H_p) \geq 0</math></b>	
$FLSC_i(n_{FC}, k : k + H_p) \leftarrow PSLC_i(n_{PC}, k : k + H_p)$	
$\bar{U}_i(n_{FC}, k : k + H_p) \leftarrow \bar{U}L_i(k : k + H_p) - PSLC_i(n_{PC}, k : k + H_p)$	
<b>end if</b>	
<b>for t=1 to <math>n_{FC}</math> (number of feasible combinations)</b>	
<b>Calculate the optimal control sequence <math>u_i(1:H_p)</math> solving <math>OP_i</math> (given by eq. (11-18)) with power constraint (given by eq. (19) equal to <math>\bar{U}_i(t, k : k + H_p)</math></b>	
$U_{pred_i}(t) \leftarrow \sum u_i(1 : H_p)$	
<b>if <math>U_{pred_i}(t) &lt; U_{pred_i}(t-1)</math> then</b>	
$FLSeq_i(1:k) \leftarrow FLSC_i(t, k : k + H_p)$	
<b>end if</b>	
<b>end for</b>	
<b>Eliminate from <math>PSLC_i</math> all the sequences that are different from <math>FLSeq_i(1:k)</math></b>	
<b>Apply <math>u_i(1)</math> (first element of the sequence <math>u_i(1:H_p)</math> resulting from <math>OP_i</math>)</b>	
<b>end for</b>	
<b>end for</b>	
<b>Remark: generically, <math>X(k : k + H_p)</math> represents a line vector (<math>1 \times H_p</math>) containing values from <math>x(k)</math> to <math>x(k + H_p)</math>, and <math>Y(p, k : k + H_p)</math> represents the line <math>p</math> of a matrix (<math>P \times H_p</math>) containing values from <math>y(p, k)</math> to <math>y(p, k + H_p)</math>.</b>	

As mentioned the algorithm is sequential, and for a better understanding of the implemented power distribution scheme, the access order is  $W_1, W_2$  and so on. Therefore, for a certain instant, is considered that  $W_1$  was the one that made the highest bid,  $W_2$  made the second highest, always sequentially until  $W_{NW}$ . In Fig. 5, the available power for  $W_1$  is given by the predicted *green* total available resource

( $\bar{U} \max_1 = U_{T_{green}}$ ) at the control horizon (21), and then the fixed consumption (20) is subtracted to  $\bar{U} \max_1$  resulting in  $\bar{U}L_i$ . As mentioned, the  $PLSC_S$  are compared inside the predictive horizon with  $\bar{U}L_i$ , and the ones that exceed it at any instant are removed, and the remaining are the  $FLSC_S$ . The  $FLSC_S$  allows us to obtain the combinations  $\bar{U}_i$ . These combinations are the power constraint (15) that are tested in

the  $OP_i$  (6). The combination that generate lower consumption,  $u_i$ , is chosen. Then, the information about the available *green* energy is passed for the next house,  $\bar{U}_{\max_i}$ .

For a generic agent  $i$  at the control horizon  $U_{T_{green}}$  represent the *green* available total resource,  $Cw_{il}$  the fixed consumption profile and  $u_{il}$  the used power to heating/cooling the space that results from the optimization program. These parameters are express by the vectors (20-22),

$$Cw_{il} = [cw_{il}(k), \dots, cw_{il}(k + H_p)]^T, \quad (20)$$

$$U_{T_{green}} = \left[ \left[ u_{T_{green}}(k) \right], \dots, \left[ u_{T_{green}}(k + H_p) \right] \right]^T, \quad (21)$$

$$u_{il} = \left[ \left[ u_{il}(k) \right], \dots, \left[ u_{il}(k + H_p) \right] \right]^T. \quad (22)$$

In the built algorithm it is considered that the access order to the *green* resource is established hourly according to bid value made in auction by each agent, and therefore, at each instant the defined access sequence must be applied. Another feature provided by the implemented system is that each house can have different hourly penalties, allowing the consumer to choose between more/less comfort and cost during the day.

The presented results were obtained with an optimization MATLAB<sup>®</sup> routine that finds a constrained minimum of a quadratic cost function that penalizes the sum of the several objectives (6).

### 3.1. One house scenario

To simplify better understand the used approach, the first results here depicted show only the shifting loads procedure for one house represented by one division with thermal disturbance ( $P_d$ ), Fig. 7 (no fixed consumption profile and storage are considered). Table 1 shows the used scenario parameters. The outdoor temperature forecast, Fig. 6, considers 90% accuracy to within +/- 2°C on the next day.

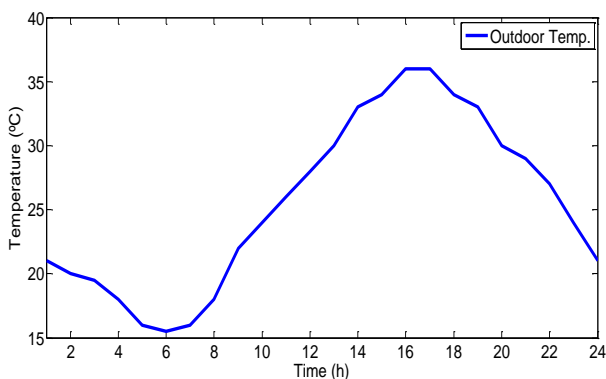


Fig. 6. Outdoor temperature forecasting ( $T_{oo}$ ).

Table 1. Scenario parameters

Parameters								
$R(^{\circ}C/kW)$	$C(kJ/^{\circ}C)$	$\Xi$	$\Psi$		$\Delta t(h)$	$H_p$	$H_c$	$T(0)(^{\circ}C)$
50	$9.2 \times 10^3$	500	500	2	1	24	24	21

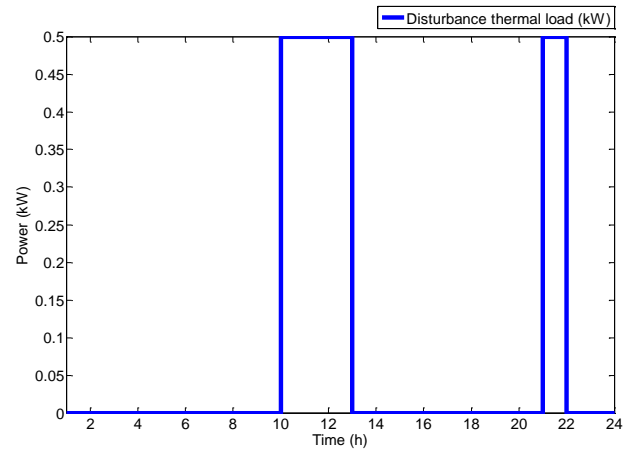


Fig. 7. Thermal disturbance forecasting ( $P_d$ ).

The loads that can be daily shifted have the characteristics present in the next Table 2, and Fig. 8 shows all the possible 56 loads combinations in the 24hours period.

Table 2. Shifted loads characteristics

Loads	$L_V(kW)$	$L_{Va}(h)$	$T_{oT}(h)$	$S_L(h)$
Load 1	3	2	8	3
Load 2	2	3	18	4

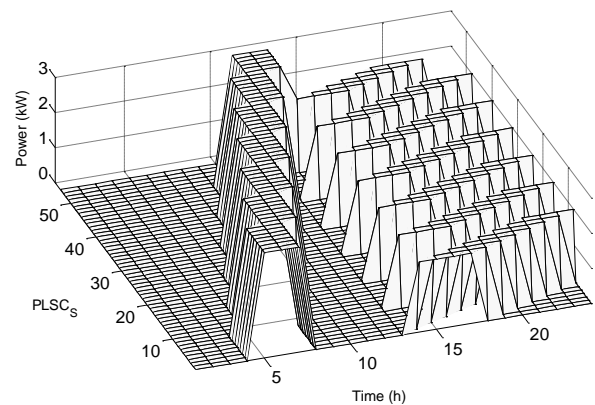


Fig. 8. Possible loads schedule combinations ( $PLSC_s$ ).

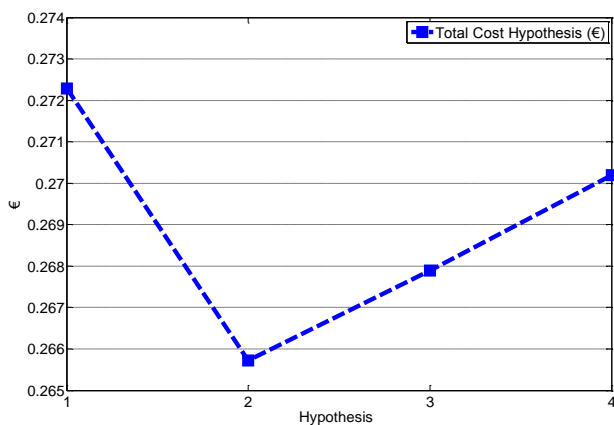
The system tests all combinations present in Fig. 8, and as mentioned above, the hypotheses that do not respect the maximum predicted *green* resource are initially discarded, and the remaining ones the  $FLSC_s$ , Table 3, are tested in (6).

The sequence  $FLSeq$ , where mostly *green* energy is consumed, the costs are lower and the indoor comfort range, is respected is found.

**Table 3.** Feasible Loads Sequence Combinations

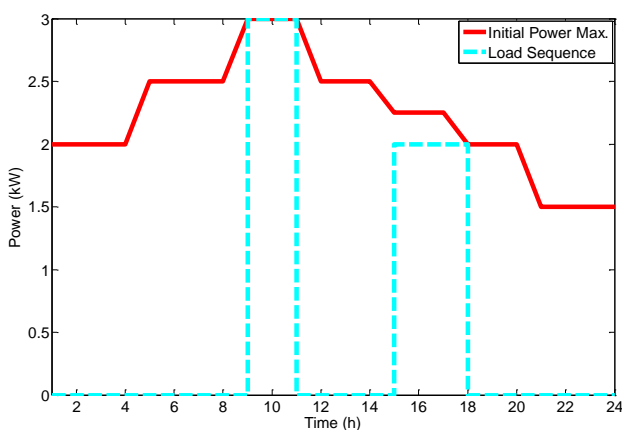
FLSC	Time (h)											
	1	2	3	4	5	6	7	8	9	10	11	12
1	0	0	0	0	0	0	0	0	3	3	3	0
2	0	0	0	0	0	0	0	0	3	3	3	0
3	0	0	0	0	0	0	0	0	3	3	3	0
4	0	0	0	0	0	0	0	0	3	3	3	0
FLSC	Time (h)											
	13	14	15	16	17	18	19	20	21	22	23	24
1	0	2	2	2	2	0	0	0	0	0	0	0
2	0	0	2	2	2	2	0	0	0	0	0	0
3	0	0	0	2	2	2	2	0	0	0	0	0
4	0	0	0	0	2	2	2	2	0	0	0	0

In Fig. 9 are the total energy costs of the  $FLSC_S$  shown in Table 3, and can be seen that the chosen sequence is the less expensive.



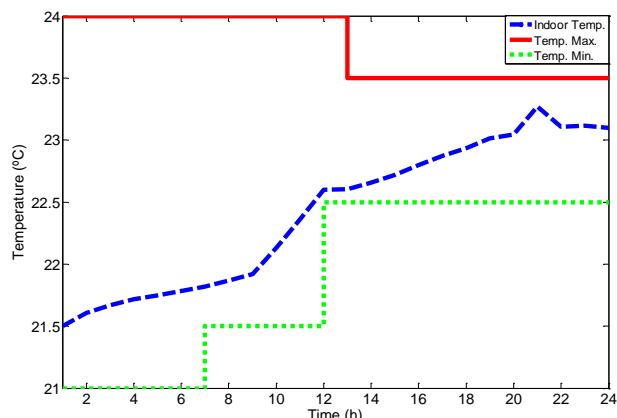
**Fig. 9.** Total energy costs of  $FLSC_S$ .

Figure 10 show the chosen load sequence,  $FLSeq$ , and the available *green* energy to allocate the loads.



**Fig. 10.** Maximum available *green* energy and chosen sequence

In order to minimize the energy costs by consuming only *green* resource, the implemented algorithm chooses the gaps that fit properly in the maximum available *green* energy.



**Fig. 11.** Indoor temperature and comfort.

The comfort limits varies during the 24h period, and Fig. 11 shows that the indoor temperature is always maintained inside the comfort limits being the optimization problem able to respect the temperature and power constraint Fig.12.

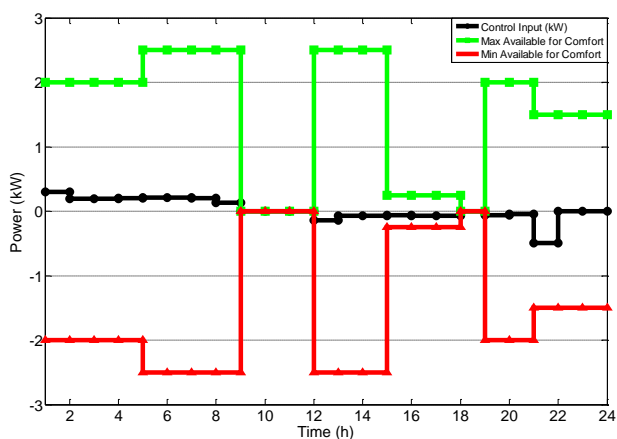


**Fig. 12.** Used power to heat/cool the space (Control input) and the maximum *green* resource available for comfort.

The periods between 9-11h and 15-18h are extremely demanding, all *green* energy is consumed by the shifted loads, with no remaining one for comfort proposes. Although, Fig. 11 shows that in that periods the algorithm choose to not use the *red* resource and, taking advantage of the prediction horizon, pre-heat or pre-cool the spaces when only renewable resource is available.

### 3.2. Distributed scenario

It is considered that all houses are represented by one division and have the same outdoor temperature presented in Fig. 6. The thermal characteristics, Table 4, load disturbances profile and comfort temperature bounds are different for all houses. The batteries capacity is 3kWh. To incentive the clean resource consumption, it is considered that the *green* energy price per kWh has a maximum auction value (0.09€/kWh) always cheaper than the *red* energy price (0.17€/kWh). In all houses, the fixed consumption profile



$Cw_1$ ,  $Cw_2$ , and  $Cw_3$ , is known within a 24h period, and represent the base in the power profile in Fig. 15, 16, 17. Table 5 shows the bid value for each one of the priority levels that, as mentioned, are established according the fixed consumption profile.

**Table 4.** Distributed scenario parameters

Parameter	A <sub>1</sub>	A <sub>2</sub>	A <sub>3</sub>	Units
$R_{eq}$	50	25	75	°C/kW
$C$	$9.2 \times 10^3$	$4.6 \times 10^3$	$11 \times 10^3$	kJ/°C
$\Xi$	100	100	300	-
$\Psi$	500	200	300	-
$\Phi$	2	2	2	-
$\Delta t$	1	1	1	h
$H_P$	24	24	24	-
$T(\theta)$	21	23	24	°C

**Table 5.** Bid value for each consumption level by house

Consumption	Priority Level	House 1	House 2	House 3
0-1 kW	1	$2/5 \times 0.09$	$3/5 \times 0.09$	$1/2 \times 0.09$
1-2 kW	2	$7/10 \times 0.09$	$4/5 \times 0.09$	$2/3 \times 0.09$
>2 kW	3	$8.5/10 \times 0.09$	$9/10 \times 0.09$	$3/4 \times 0.09$

**Table 6.** Shifted loads characteristics for distributed scenario

House	Loads	$L_V$ (kW)	$L_{Va}$ (h)	$T_{oT}$ (h)	$S_L$ (h)
1	Load 1	1	2	7	1
	Load 2	2	4	18	2
2	Load 1	2	3	9	1
	Load 2	2	2	21	2
3	Load 1	3	3	8	1
	Load 2	3	3	13	1

The thermal disturbance profiles are presented in Fig. 13.

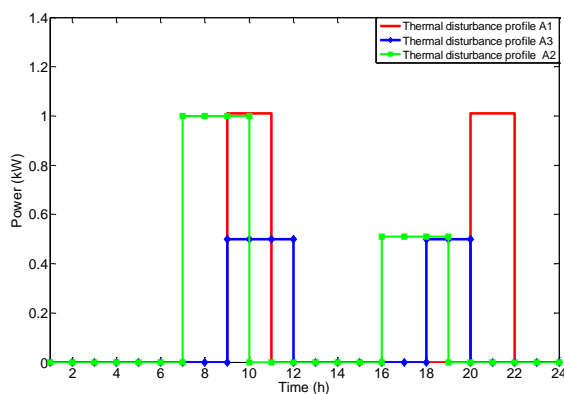


**Fig. 13.** Thermal disturbance profile of each house ( $P_{d1}$ ,  $P_{d2}$  and  $P_{d3}$ ).

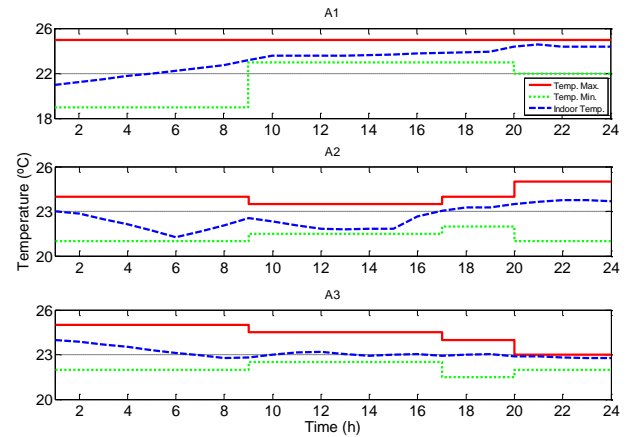


**Fig. 14.** A<sub>1</sub>, A<sub>2</sub> and A<sub>3</sub> indoor temperature and their constraints.

As mentioned, the external thermal disturbance profile presented in Fig. 13 is known within a 24 hour period, and is related with thermal loads generated by occupants, direct sunlight, electrical devices or doors and windows aperture to recycle the indoor air

In Fig. 14, it can be seen that the comfort constraints are respected, the indoor temperature is always inside the comfort zone in all houses. Taking advantage of the predictive knowledge of the thermal disturbance and making use of the space thermal storage, it can also be seen that in all houses the MPC treats the indoor temperature before the thermal disturbance beginning.

In Fig.15 it can be seen that the shifted loads were located in zones with mostly *green* energy available. Note that when the used power is above the daily maximum *green* available resource, means that the *red* resource was consumed. The used power to heat/cool the space is maintained inside the constrained bounds and when the *green* energy is null the used power is also null, Fig. 16.

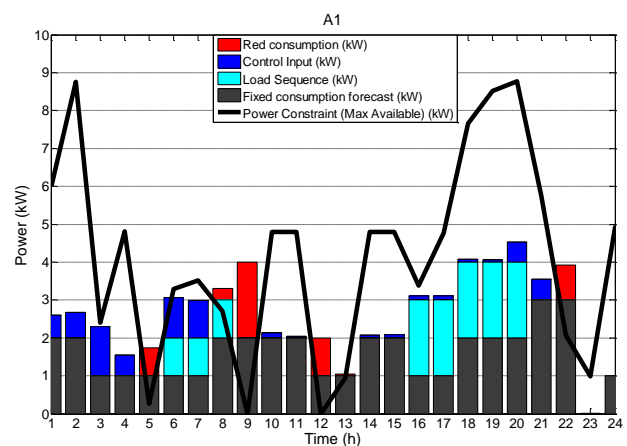


**Fig. 15.** Power profile A<sub>1</sub>.

Remark that, for example, at time instant  $t=7$ , three different types of energy utilization are used. The base, in dark grey, is fulfil with the fixed consumption, above is the shifted load and on top is the used power for comfort. In this instant the total consumption is maintained within the power constraint. On the other hand, at instant  $t=9$ , with no

available *green* power, all the fixed consumption of 2kW is made with *red* resource.

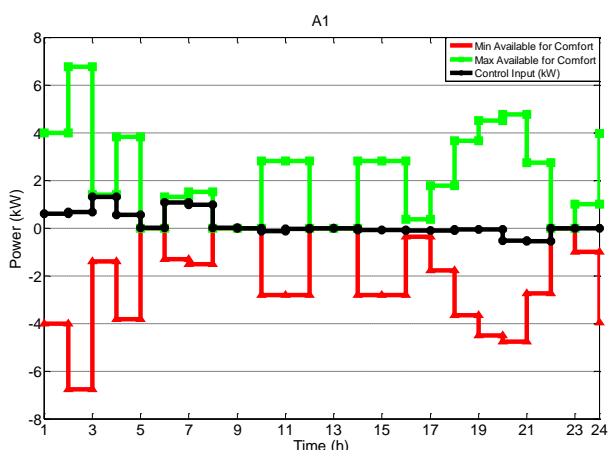


Fig. 16. Control input profile A<sub>1</sub>.

In Fig.17 it can be seen that the shifted loads of house 2 were mostly located in zones with mostly *green* energy available.

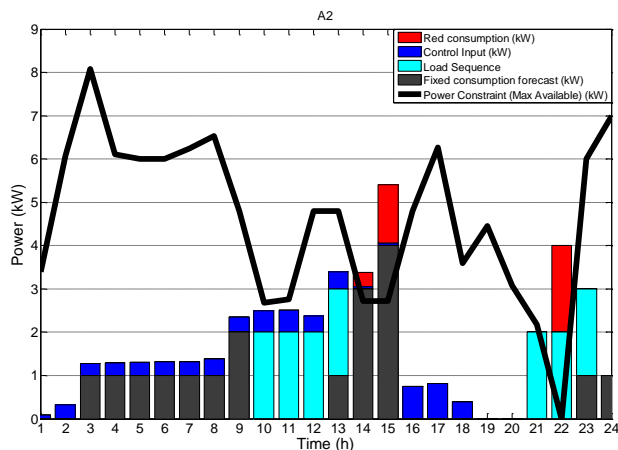


Fig. 17. Power profile A<sub>2</sub>.

The used power to heat/cool the space is always maintained inside the constrained bounds been the clean resource consumed only when is available. Note that when the used power to satisfy all the demand is above the daily maximum *green* available resource, means that the *red* resource was consumed, Fig 17.

Figure 19 shows that the chosen  $FLSeq_3$  is located here the consumption of *red* resource is obliged. Due the access order imposed by the auction, the maximum available energy may change hourly, and by this fact the available resource prediction is not as effective as with one house only. Also, the  $SL=1$  of both loads of house 3 (Table 6), is obvious a conditionality and an extra restriction on our optimization algorithm.

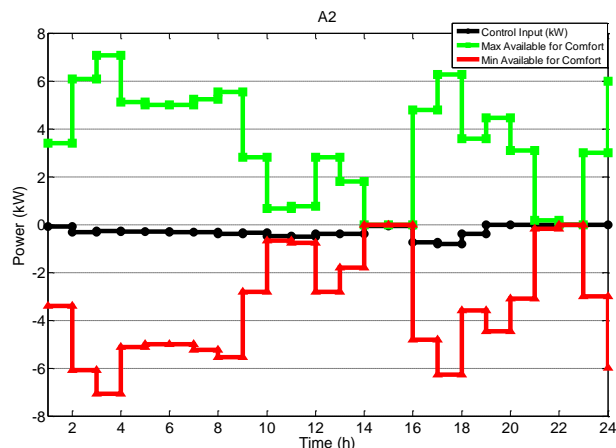


Fig. 18. Power profile A<sub>2</sub>.

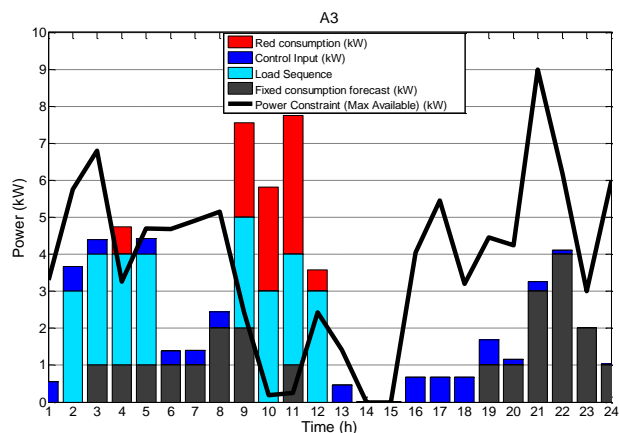


Fig. 19. Power profile A<sub>3</sub>.

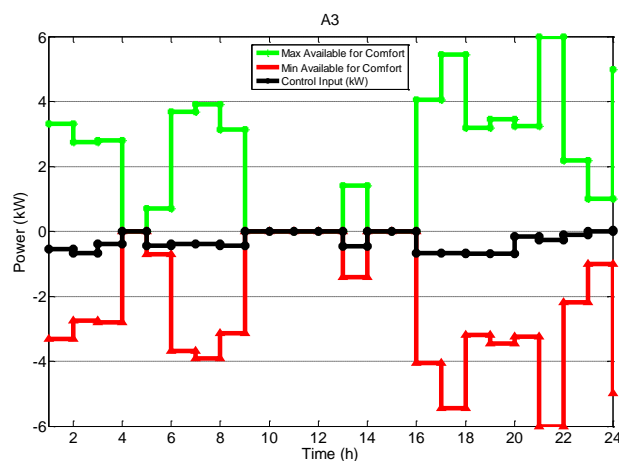


Fig. 20. Power profile A<sub>3</sub>.

The power constrained bounds are respected been the consumed made only when the clean resource is available, Fig. 20. The batteries profile during the 24h period is show in Figure 21. It can be seen that in the most demanding periods, the energy available in the batteries provide a useful energy support. Figure 22 demonstrates the advantage of the auction. For each one of the houses it can be seen that the “Real Cost” is much lower than the cost of not to bid in auction and only consume the *red* resource “Red Cost” at a higher fixed price.

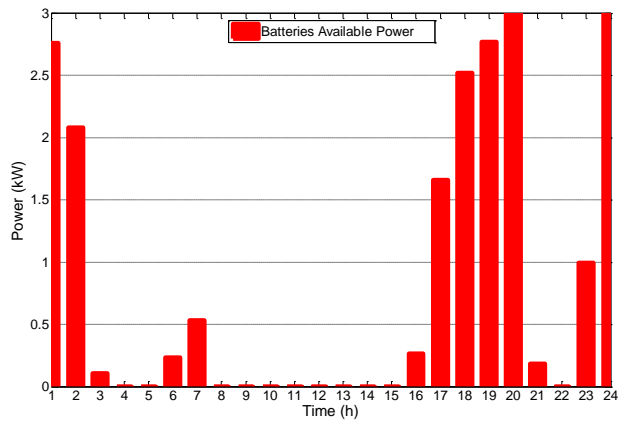


Fig. 21. Batteries profile.

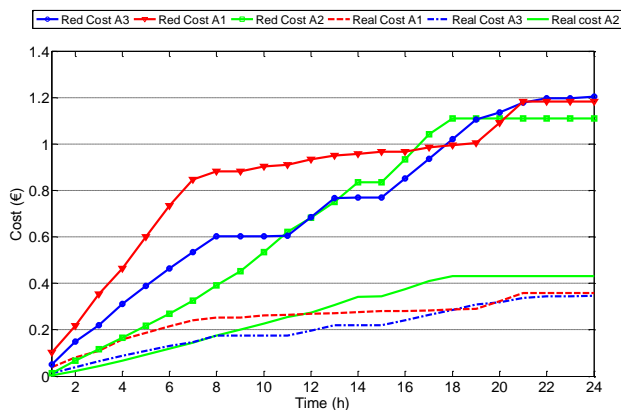


Fig. 22. Consumption costs.

In this paper, a distributed MPC control integrative solution was validated in order to provide thermal house comfort in an environment with strong presence of intermittent/limited renewable energy sources. The approach boils up to a control problem of multiple subsystems (multi-agent) subject to coupled constraint solved as a sequence of QP optimization problems for each time instant.

The approach shows that distributed predictive control provides house comfort within a DSM policy, based in a price auction and the rescheduling of appliance loads, is a valid methodology to achieve less consumption and price reduction. The approach is more effective as wide as the period during which the loads are allowed to sliding and consequently allocating in the most favourable zone.

Future work will focus in a distributed approach where each agent has a daily cash credit to spend in energy. According to the selected indoor temperature, weather forecasts, the disturbances forecasts and available power and credit, the agent must decide when some house appliances are turned on or off. It also remains to future investigations to add negotiation iteration techniques between agents to improve decision making.

### Abbreviations/Nomenclature

$A_O$	access order to <i>green</i> resource
$B_{cV}$	batteries capacity value
$B_{Vi}$	bid value at instant $i$
$Cw_{il}$	fixed consumption of house $w_i$
DMPC	Distributed Model Predictive Control
DSM	Demand-Side Management
FLSC <sub>S</sub>	feasible load schedule combinations
FLSeq	final load sequence
$L_V$	load value
$L_{Va}$	load value duration
MAS	Multi Agent System
MPC	Model Predictive Control
PLSC <sub>S</sub>	possible loads schedule combinations
SGs	Smart Grids
$S_L$	sliding level
TCA	thermal control area
$T_{oT}$	turned on time

### References

- [1] Available on: <http://www.storepet-fp7.eu/project-overview>.
- [2] I. Korolija, L. Marjanovic-Halburd, Y. Zhang, and V. I. Hanby, "Influence of building parameters and HVAC systems coupling on building energy performance," *Energy Build.*, vol. 43, no. 6, pp. 1247–1253, Jun. 2011.
- [3] U.S Energy Information Administration: Available on: <http://www.eia.gov/>.
- [4] P. Perrod, R. Critchley, E. Catz, M. Bazargan, "New participants in SmartGrids and associated challenges in the transition towards the grid of the future", *IEEE Bucharest Power Tech Conference*, Bucharest. Page(s): 1 – 5, 2009.
- [5] A. Kosek, G. Costanzo, H. Bindner and O. Gehrke, "An overview of demand side management control schemes for buildings in smart grids", *IEEE International Conference on Smart Energy Grid Engineering (SEGE)*, Oshawa, Canada. 2013.
- [6] C. Chen, Y. Zhu, Y. Xu, "Distributed generation and Demand Side Management", *Proceedings of International Conference on Electricity Distribution (CICED) 2010*.
- [7] T. Luo, G. Ault, S. Galloway, "Demand Side Management in a highly decentralized energy future", *Proceedings of 45<sup>th</sup> International Universities Power Engineering Conference (UPEC)*, 2010.
- [8] D. Callaway, "Tapping the energy storage potential in electric loads to deliver load following and regulation,

- with application to wind energy”, *Energy Conversion and Management*. Pp 1389–1400. 2009.
- [9] V. Molderink, V. Bakker, M. Bosman, J. Hurink and G. Smith, “Management and Control of Domestic Smart Grid Technology”, *IEEE Transactions on Smart Grid*, Vol. 1, Issue: 2, 2010, Page(s): 109 – 119.
- [10] F. Saffre and R. Gedge, “Demand-Side Management for the Smart Grid”, *Network Operations and Management Symposium Workshops (NOMS Wksp)*, 2010 IEEE/IFIP, Page(s): 300 – 303I.
- [11] V. Hamidi, F. Li and F. Robinson, “The effect of responsive demand in domestic sector on power system operation in the networks with high penetration of renewable”, *IEEE Power and Energy Society General Meeting - Conversion and Delivery of Electrical Energy in the 21st Century*, Page(s): 1 – 8. 2008.
- [12] S. Gottwalt, W. Ketter, C. Block, J. Collins, and C. Weinhardt, “Demand side management simulation of household behaviour under variable prices”, *Energy Policy*, Vol. 39, no. 12, pp. 8163 – 8174, 2011.
- [13] A. Di Giorgio, L. Pimpinella, F. Liberati, “A Model Predictive Control Approach to the Load Shifting Problem in a Household Equipped with an Energy Storage Unit”, *20th Mediterranean Conference on Control and Automation (MED 2012)*, Barcelona, 3-6 July 2012.
- [14] E. Matallanas, M. Castillo-Cagigal, A. Gutierrez, F. Monasterio Huelin, E. Caamano-Martin, D. Masa, and J. Jimenez-Leube, “Neural network controller for Active Demand-Side Management with PV energy in the residential sector”, *Applied Energy*, Vol. 91, no. 1, pp.90 – 97, 2012.
- [15] P. Moroşan, R. Bourdais, D. Dumur and J. Buisson, “Building temperature regulation using a distributed model predictive control”, *American Control Conference (ACC)*. Pp. 3174 – 3179. 2010.
- [16] Y. Ma, A. Kelman, A. Daly and F. Borrelli, “Predictive Control for Energy Efficient Buildings with Thermal Storage”, *IEEE Control System Magazine*, February 2012. Vol 32, n°1, pp. 44 – 64.
- [17] R. Balan, S. Stan, C. Lapusan, “A Model Based Predictive Control Algorithm for Building Temperature Control”, *3<sup>rd</sup> IEEE International Conference on Digital Ecosystems and Technologies, DEST '09*, pp. 540 – 545. 2009.
- [18] R. Freire, G. Oliveira, N. Mendes, “Non-linear Predictive Controllers for Thermal Comfort Optimization and energy Saving.”, *IFAC WS ESC'06 Energy Saving Control in Plants and Buildings*, pp. 87-92. 2006.
- [19] F. Barata J. Igreja and R. Neves-Silva “Model Predictive Control for Thermal House Comfort with Limited Energy Resources”, *Proceedings of the 10th Portuguese Conference on Automatic Control, Madeira, July 2012*, pp. 146-151.
- [20] M. Maasoumy, M. Razmara, M. Shahbakhti, and a. S. Vincentelli, “Handling model uncertainty in model predictive control for energy efficient buildings,” *Energy Build.*, vol. 77, pp. 377–392, Jul. 2014.
- [21] J. Cigler, P. Tomáško, and J. Široký, “BuildingLAB: A tool to analyze performance of model predictive controllers for buildings,” *Energy Build.*, vol. 57, pp. 34–41, Feb. 2013.
- [22] R. Negenborn, *Multi-Agent Model Predictive Control with Applications to Power Networks*. In: PhD Thesis, Technische Universiteit Delft. Nederland, 2007.
- [23] R. Scattolini, “Architectures for distributed and hierarchical Model Predictive Control – A review”, *Journal of Process Control*, Vol.19, pp 723–731. 2009.
- [24] V. Chandan and A. G. Alleyne, “Decentralized predictive thermal control for buildings,” *J. Process Control*, pp. 1–16, Apr. 2014.
- [25] P. Trodden and A. Richards, “Distributed model predictive control of linear systems with persistent disturbances”, *International Journal of Control*, Vol. 83, No. 8, August 2010, pp. 1653–1663. 2010.
- [26] T. Keviczky, F. Borrelli, and G. Balas, “Decentralized Receding Horizon Control for Large Scale Dynamically Decoupled Systems”, *Automatica*, Vol. 42, pp. 2105–2115. 2006.
- [27] Q. Xu, X. Jia, L. He, “The control of Distributed Generation System using Multi-Agent System”, *International Conference On Electronics and Information Engineering (ICEIE)*, Vol. 1 On page(s): V1-30 - V1-33. 2010.
- [28] K. Mets, M. Strobbe, T. Verschueren, T. Roelens, F. Turck, C. Develder, “Distributed Multi-Agent Algorithm for Residential” *Energy Management in Smart Grids*”, *Proceedings of IEEE IFIP Network Operations and Management Symposium*, pp.435-443. 2012.
- [29] M. Pipattanasomporn, H. Feroze, S. Rahman, “Multi-agent systems in a distributed smart grid: Design and implementation”, *PSCE '09, IEEE/PES Power Systems Conference and Exposition*. 2009.
- [30] F. Barata and R. Neves-Silva, “Distributed model predictive control for thermal house comfort with auction of available energy”, *Proceedings of International Conference on Smart Grid Technology, Economics and Policies (SG-TEP 2012)*. 2012.
- [31] I. Hazyuk, C. Ghiaus, D. Penhouet, “Optimal temperature control of intermittently heated buildings using Model Predictive Control: Part I - Building modeling”, *International Journal Building and Environment*, Vol. 51, pp. 379-387. 2012.
- [32] B. Bequette, *Process Control, Modeling, Design and Simulation*, Prentice Hall, pp.58. 2003.

**Annexes**

heating/cooling sources, obtained using the thermal model of Section 2.2.

Equation (23) represents the continuous space-state model for a whole house with  $Nd$  divisions and  $Nd$

$$\begin{bmatrix} \dot{T}_{i1} \\ \dot{T}_{i2} \\ \vdots \\ \dot{T}_{iNd} \end{bmatrix} = \begin{bmatrix} \frac{1}{R_{eqi1}C_{i1}} & \frac{1}{R_{i12}C_{i1}} & \dots & \frac{1}{R_{i1Nd}C_{i1}} & \dots & \dots \\ & \frac{1}{R_{i21}C_{i2}} & \dots & \frac{1}{R_{i2Nd}C_{i2}} & \dots & \dots \\ & \vdots & \dots & \vdots & \dots & \dots \\ & \frac{1}{R_{iNd1}C_{iNd}} & \dots & \frac{1}{R_{iNd2}C_{iNd}} & \dots & \dots \\ \dots & \dots & \dots & \dots & \dots & \dots \\ \dots & \dots & \dots & \dots & \dots & \dots \end{bmatrix} \begin{bmatrix} T_{i1} \\ T_{i2} \\ \vdots \\ T_{iNd} \end{bmatrix} + \begin{bmatrix} \frac{T_{out} + \frac{Pd_{i1}}{C_{i1}}}{R_{eqi1}C_{i1} + C_{i1}} \\ \frac{T_{out} + \frac{Pd_{i2}}{C_{i2}}}{R_{eqi2}C_{i2} + C_{i2}} \\ \vdots \\ \frac{T_{out} + \frac{Pd_{iNd}}{C_{iNd}}}{R_{eqiNd}C_{iNd} + C_{iNd}} \end{bmatrix} \begin{bmatrix} \frac{1}{C_{i1}} & 0 & \dots & 0 \\ 0 & \frac{1}{C_{i2}} & \dots & \vdots \\ \vdots & \vdots & \ddots & 0 \\ 0 & \dots & 0 & \frac{1}{C_{iNd}} \end{bmatrix} \begin{bmatrix} u_{i1} \\ u_{i2} \\ \vdots \\ u_{iNd} \end{bmatrix} \quad (23)$$